Stem Cell Reports
Article

ISSCR

OPEN ACCESS

# Characterization and Transplantation of CD73-Positive Photoreceptors Isolated from Human iPSC-Derived Retinal Organoids

Giuliana Gagliardi,[1] Karim Ben M'Barek,[2] Antoine Chaffiol,[1] Amélie Slembrouck-Brec,[1] Jean-Baptiste Conart,[1] Céline Nanteau,[1] Oriane Rabesandratana,[1] José-Alain Sahel,[1,3,4] Jens Duebel,[1] Gael Orieux,[1] Sacha Reichman,[1] and Olivier Goureau[1,*]

[1]Institut de la Vision, Sorbonne Université, INSERM, CNRS, 17, Rue Moreau, Paris 75012, France
[2]INSERM U861, UEVE, CECS, AFM, Institute for Stem Cell Therapy and Exploration of Monogenic Diseases, Corbeil-Essonnes 91100, France
[3]CHNO des Quinze-Vingts, DHU Sight Restore, INSERM-DHOS CIC, Paris 1423, France
[4]Department of Ophthalmology, University of Pittsburgh School of Medicine, Pittsburgh, PA 15213, USA
*Correspondence: olivier.goureau@inserm.fr
https://doi.org/10.1016/j.stemcr.2018.07.005

## SUMMARY

Photoreceptor degenerative diseases are a major cause of blindness for which cell replacement is one of the most encouraging strategies. For stem cell-based therapy using human induced pluripotent stem cells (hiPSCs), it is crucial to obtain a homogenous photoreceptor cell population. We confirmed that the cell surface antigen CD73 is exclusively expressed in hiPSC-derived photoreceptors by generating a fluorescent cone rod homeobox (Crx) reporter hiPSC line using CRISPR/Cas9 genome editing. We demonstrated that CD73 targeting by magnetic-activated cell sorting (MACS) is an effective strategy to separate a safe population of transplantable photoreceptors. CD73+ photoreceptor precursors can be isolated in large numbers and transplanted into rat eyes, showing capacity to survive and mature in close proximity to host inner retina of a model of photoreceptor degeneration. These data demonstrate that CD73+ photoreceptor precursors hold great promise for a future safe clinical translation.

## INTRODUCTION

Retinal diseases caused by the cell death of photoreceptors (PRs) and/or supporting retinal pigment epithelium (RPE), such as age-related macular degeneration and retinitis pigmentosa, are the increasingly significant cause of incurable sight loss. Cell replacement represents a potential vision restoration strategy for advanced stage of disease with severe cell loss (Dalkara et al., 2016; Zhao et al., 2017). While RPE replacement alone may be used for specific disease indications, transplantation of PRs—as a retinal sheet or as a suspension of dissociated cells—is required after extensive PR degeneration (Jayakody et al., 2015; Santos-Ferreira et al., 2017; Zhao et al., 2017). Prior studies in animal models revealed that transplantation of post-mitotic PR precursors, isolated from mouse neonatal retinae, might be feasible (Pearson et al., 2012; Santos-Ferreira et al., 2015; Singh et al., 2013). Donor PRs derived from mouse pluripotent stem cells (PSCs) have been transplanted into the subretinal space (SRS) of different blind mice models, showing integration into the degenerating retina, differentiation into mature PRs, and formation of synaptic connections, possibly leading to partial recovery of visual function (Decembrini et al., 2014; Gonzalez-Cordero et al., 2013; Mandai et al., 2017; Santos-Ferreira et al., 2016a; Tucker et al., 2011). However, recent work has indicated that functional recovery may be achieved by transferring of cytoplasmic material from transplanted mouse PRs to remaining host PRs, rather than through real integration into the recipient outer nuclear layer (ONL) (Decembrini et al., 2017; Ortin-Martinez et al., 2017; Pearson et al., 2016; Santos-Ferreira et al., 2016b; Singh et al., 2016). It is unclear whether human PRs may also be able to transfer cytoplasmic material to host cells (Zhu et al., 2017).

The most promising source for the unlimited generation of human PRs for cell therapy is represented by human PSCs. Different protocols have been reported allowing for the differentiation of both rod and cone PRs starting from a serum-free floating culture of embryoid body-like aggregates (SFEB) (Lamba et al., 2006; Meyer et al., 2009; Osakada et al., 2008). Considerable progress has been made over the last few years with 3D retinal organoid formation from an optimized SFEB system (Mellough et al., 2015; Nakano et al., 2012; Tucker et al., 2013; Zhong et al., 2014) or from adherent human PSCs (Gonzalez-Cordero et al., 2017; Reichman et al., 2014). Some of these protocols have been recently adapted to Good Manufacturing Practice (GMP) guidelines required for the generation of transplantable cells for future clinical applications (Reichman et al., 2017; Sridhar et al., 2013; Wiley et al., 2016). Despite continuous improvements, efficiency in generating a homogeneous cell population of post-mitotic PR precursors, corresponding to the appropriate donor cell population for cell therapy, remains to be addressed. Ensuring safety is of particular importance; transplantable cells must be devoid of mitotically active cells or residual undifferentiated PSCs that could be teratogenic (Tucker et al., 2011). As genetic engineering or viral labeling of the cells are not suitable for clinical applications, several studies have

been focusing on the identification of cell surface markers characterizing precursor and mature PRs derived from human induced pluripotent stem cells (hiPSCs) and in human retina (Kaewkhaw et al., 2015; Lakowski et al., 2018; Welby et al., 2017). However, low levels of both purity and cell yields resulting from the separation approaches used so far require further optimization, representing a challenge for future applications.

Using our GMP-compliant retinal differentiation protocol (Reichman et al., 2017), we have demonstrated that PRs express the cell surface antigen CD73, previously described for the enrichment of mouse PSC-derived PRs (Lakowski et al., 2015; Santos-Ferreira et al., 2016a). In this study, we reported a complete characterization of CD73+ cells during maturation of hiPSC-derived retinal organoids and we demonstrated that the simple CD73-based magnetic-associated cell sorting (MACS) results in selection of PRs. Transplantation of isolated CD73+ PRs in a rat model of retinal degeneration supported the usefulness of our separation strategy, which could be implemented for the development of stem cell-based therapy to treat retinal diseases due to PR cell death.

## RESULTS

### Expression of CD73 in hiPSC-Derived Retinal Organoids

We first sought to determine the expression of the *NT5E* gene coding for the surface antigen CD73 during the maturation of hiPSC-derived retinal organoids, in floating culture conditions, based on our retinal differentiation protocol (Reichman et al., 2017). qRT-PCR analysis showed that *NT5E* (CD73) starts to be expressed at day 50 (D50); this expression sharply increases until 150 days of differentiation and is maintained in organoids at later stages of maturation. As expected, expression levels of PR-specific genes *CRX* and *RECOVERIN* (*RCVRN*) were also increased, with an earlier peak of induction around D100 (Figure 1A). CD73 was present in post-mitotic cells (Ki67–) committed in the PR lineage (Figure S1). PR precursors in retinal organoids could further differentiate in all PR subtypes, rods, and red/green and blue cones, as shown by the increased expression of rhodopsin (*RHO*), red/green opsin (*OPN1LW/MW*), and blue opsin (*OPN1SW*), respectively (Figure 1B). Evaluation of CD73 expression by flow cytometry indicated that the percentage of CD73+ cells steadily increased from 7% ± 12% at D85 to 55% ± 2% at D200 of differentiation (Figure 1C, n = 10 organoids from N ≥ 3 differentiations, $^{**}p < 0.01$, Kruskal-Wallis test). Therefore, targeting the CD73+ cell population at different time of differentiation should result in isolating populations of either precursor or mature PRs (Figure 1D).

To evaluate if timing of CD73 expression was dependent on the hiPSC line used for the generation of the retinal organoids, we carried out additional characterization studies with another hiPSC line derived from adult Müller glial cells. Furthermore, to easily identify the entire PR population within the retinal organoids, we used this iPSC line to generate, using the CRISPR-Cas9 system, a fluorescent *CRX* hiPSC reporter line, in which a nuclear form of the fluorescent protein mCherry under the control of the mouse Crx promoter (Furukawa et al., 2002) was inserted into the AAVS1 site (Figure S2A). We selected a puromycin-resistant clone (CRX-c2), carrying a copy of the insert in both AAVS1 locus (Figure S2B) for further retinal differentiation. qRT-PCR analysis of *NT5E* and PR-specific gene expression in retinal organoids from AAVS1:*CrxP*_H2BmCherry hiPSC line (Figures S2C and S2D) led to similar results obtained on organoids from hiPSC line 2 (Figures 1A and 1B). In whole retinal organoids, endogenous mCherry signal was visible by D49 and it allowed tracing the differentiating mCherry+ PRs (Figure S2E). Immunostaining of sections from D100 organoids confirmed the expected nuclear localization of mCherry, due to the presence of the Histone-2B (H2B) sequence (Figure S2F). By combining whole-mount immunostaining for CRX and a clearing procedure 3DISCO (Belle et al., 2014) on D75 organoids, we showed that mCherry expression was restricted to CRX+ cells in the entire organoid (Figures 1E and S2F; Video S1), demonstrating the specificity of the mouse Crx promoter in the human context. The presence of both CONE ARRESTIN (hCAR)+/mCherry+ cells and RHODOPSIN+/mCherry+ cells identified by immunostaining (Figure S2G) confirmed that mCherry+ cells were both cone and rods. Importantly, CD73 expression was restricted to mCherry+ cells both in retinal organoid sections (Figure 1F) and in dissociated cells from organoids, where all the RECOVERIN+ cells presented a mCherry+ nucleus (Figure 1G).

### Enrichment of PRs by MACS Based on Expression of CD73 in Dissociated Retinal Organoid Cells

Since we aimed at separating the PR population from organoids by targeting CD73, we developed a protocol based on the magnetic labeling of CD73+ cells, previously used to obtain PR enrichment from post-natal mice (Eberle et al., 2011). Efficiency of the MACS process was evaluated by flow cytometry using a PE-conjugated CD73 primary antibody on dissociated retinal organoids older than D100 of differentiation, because MACS at earlier stages did not lead to a satisfactory enrichment of CD73+ cells (data not shown). We showed that the MACS-positive fraction contained 87% ± 7% of CD73+ cells (n = 20 organoids, N = 3 differentiations; Figure 2A), a rate of enrichment consistent with previously published results from

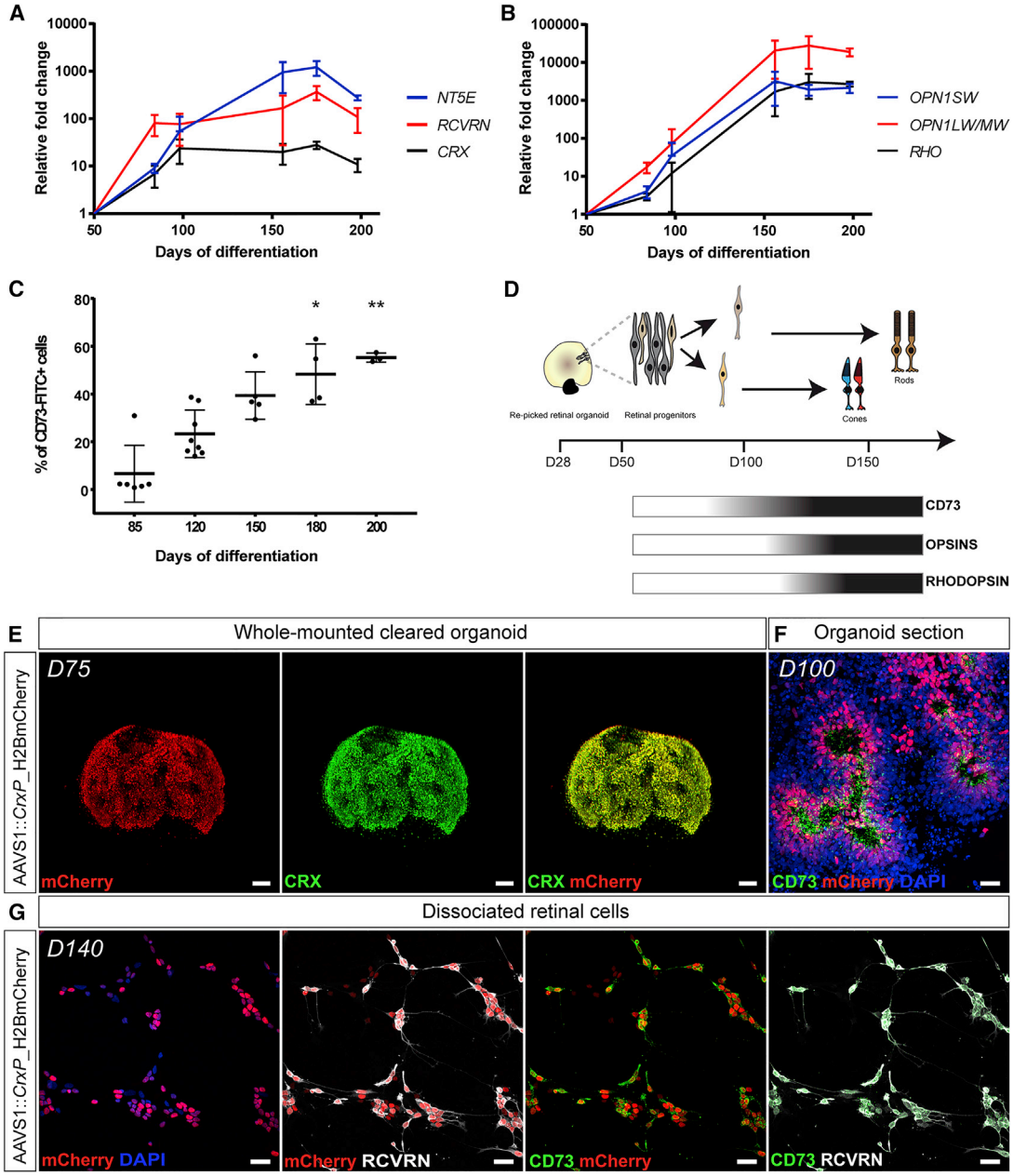


**Figure 1. Analysis of CD73 Expression in hiPSC-Derived Retinal Organoids**

(A and B) qRT-PCR analysis of *NT5E* (coding for CD73) and PR markers during differentiation between D50 and D200 (mean ± SD; n = 5 organoids from N = 3 differentiations per time point). Gene expression at each time point is indicated relative to organoids at D50.

(C) Percentage of CD73+ cells in organoids between D85 and D200 of differentiation analyzed by flow cytometry using CD73-FITC antibody (mean ± SD; n = 10 organoids from N ≥ 3 differentiations D85 versus D180 *p < 0.05, D85 versus D200 **p < 0.01, multiple comparisons Kruskal-Wallis test).

(D) Schematic summarizing temporal expression of CD73 and mature PR markers in organoids.

(E) Endogenous mCherry staining (red) and CRX immunolabeling (green) on solvent-cleared D75 organoid generated from the AAVS1:*CrxP*_H2BmCherry hiPSC line.

(F) Immunostaining showing the expression of CD73 in mCherry+ PRs in section of D100 AAVS1:*CrxP*_H2BmCherry retinal organoid.

(G) Dissociated mCherry+ cells (red) from D140 AAVS1:*CrxP*_H2BmCherry retinal organoids co-expressing RECOVERIN (gray) and CD73 (green). Nuclei were counterstained with DAPI (blue) in the first left panel.

Scale bars, 100 μm (E), 25 μm (F and G).

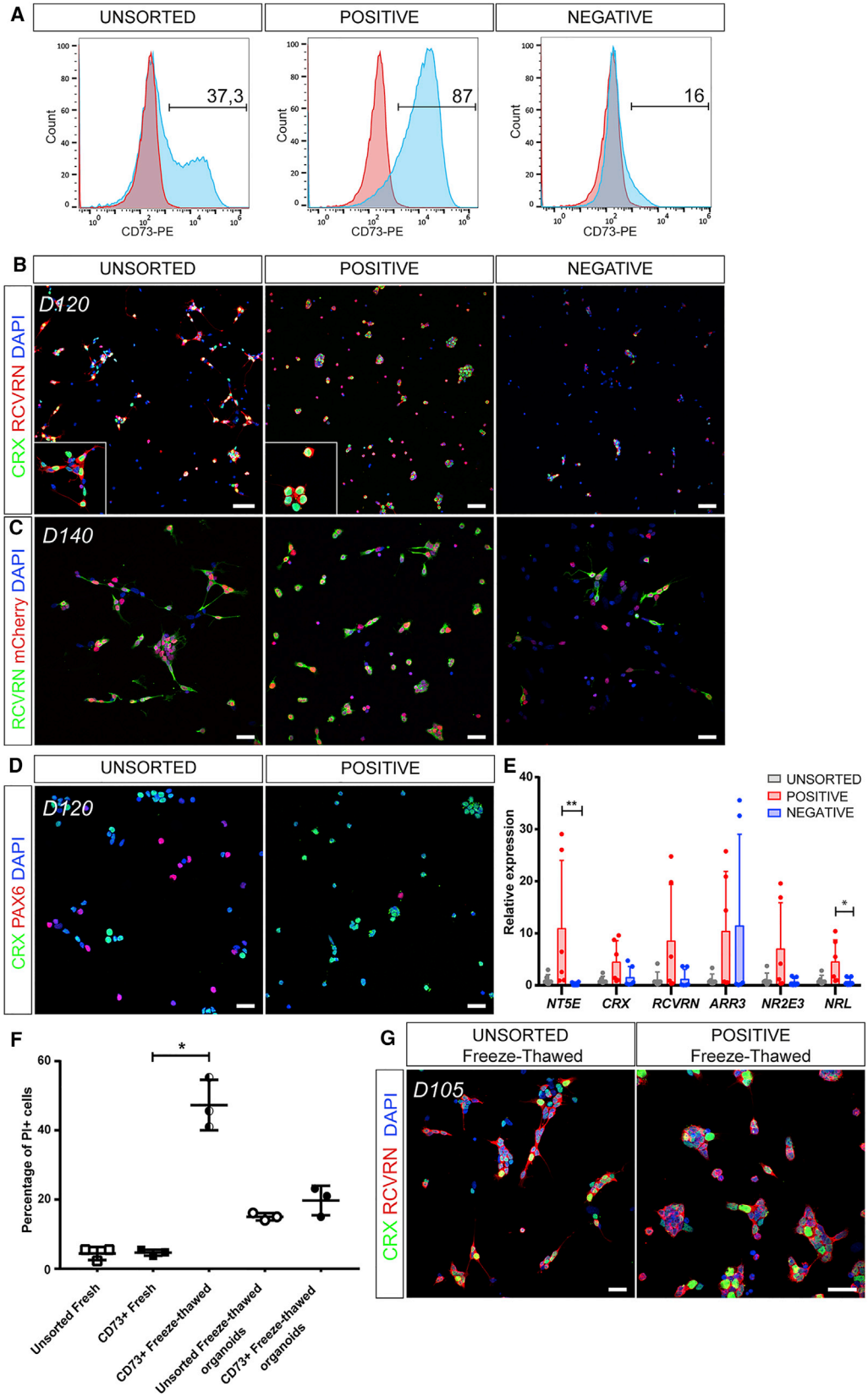


(legend on next page)

post-natal mouse retinae or retinal cells from mPSCs (Eberle et al., 2011; Santos-Ferreira et al., 2016a). CD73+ fractions from D120 organoids revealed relative enrichment in CRX+/RECOVERIN+ cells (66% ± 15%) compared with the unsorted fractions (32% ± 7%) (Figure 2B), with the percentage of CRX+ cells being increased from 53% ± 10% in unsorted fractions to 79% ± 11% in CD73+ fractions (n = 10 images, N = 3 differentiations, ****p < 0.0001, two-way ANOVA with Tuckey's multiple comparisons test). MACS for CD73 was performed on D140 organoids generated from the AAVS1:*CrxP*_H2BmCherry hiPSC line to validate the efficacy and the reproducibility of our separation strategy. As expected, almost all CD73+ cells in the MACS-positive fraction displayed mCherry+ nuclei (98% ± 0.7%, n = 12 images, N = 3 differentiations), as well as RECOVERIN-positive immunostaining (Figure 2C). A qualitative depletion of mCherry+ cells was observed in the CD73– fraction, as opposed to the clear enrichment observed in the CD73+ fraction. Immunostaining for PAX6, corresponding to horizontal, amacrine, and retinal ganglion cells in retinal organoids (Reichman et al., 2017), demonstrated that PAX6+ cells constituted an abundant population in unsorted fractions from D120 organoids, while the MAC-sorted CD73+ cell population contained very few PAX6+ cells (Figure 2D). qRT-PCR analysis confirmed that *NT5E* expression level was significantly higher in CD73+ cells than in CD73– cells at D120 (Figure 2E). Other markers of PR specification were expressed at increased levels in CD73+ cells (Figure 2E). The relatively modest increase of CRX+ cells could be due to the ontogenetic stage of organoids, where the differentiating CRX+/CD73– cells present in D120 organoids were still present in the negative fractions. Ratios of gene expression levels between CD73+ and CD73– fractions confirm increased expression in CD73+ cells for the PR genes analyzed (Figure S3A). All together, these data support the use of CD73 as a marker of both differentiating cone and rod PRs and validate the MACS of CD73+ cells around D120 of differentiation as an efficient strategy to obtain a homogeneous and viable population of hiPSC-derived PR precursors.

With the perspective of developing a cell therapy product, we have tested the possibility to cryopreserve the isolated population of CD73+ cells directly after MACS. The evaluation of cell viability in freeze-thawed CD73+ cells by flow cytometry using propidium iodide (PI) revealed that 47% ± 7% of the cells are apoptotic (PI+) after thawing (compared with 4.6% ± 0.9% in fresh CD73+ cells, n = 15 organoids, N = 3 differentiations, *p < 0.05, Kruskal-Wallis test) (Figure 2F). Having already developed a simple cryopreservation procedure of whole retinal organoids with no impact on CD73 expression (Reichman et al., 2017), we tested whether freeze-thawed organoids could still represent a source for MACS of viable CD73+ PR precursors. Retinal organoids, frozen at D90 of differentiation, were thawed and put back into floating cultures for an additional 2 weeks before performing MACS. In these conditions, MACS of CD73 cells still resulted in efficient enrichment of PR precursors, as shown by co-immunostaining with CRX and RECOVERIN (Figure 2G). The assessment of cell viability demonstrated that freeze-thawing resulted in a small, but not significant, increase in the number of apoptotic cells from 4.4% ± 1.9% to 15% ± 1% of PI+ cells in unsorted fractions from fresh and freeze-thawed organoids respectively (n = 15 organoids, N = 3 differentiations). MACS alone did not significantly affect cell viability in any condition: 4.4% ± 1.9% compared with 4.6% ± 0.9% and 15% ± 1% to 19.7% ± 4.2% of PI+ cells for fresh and freeze-thawed organoids respectively (n = 15 organoids, N = 3 differentiations) (Figure 2F).

### Maturation of CD73+ PRs

To analyze more deeply the cell identity of CD73+ cells, MACS for CD73 was performed on 200-day-old retinal

**Figure 2. Selection of hiPSC-Derived PRs by Targeting of CD73**

(A) Representative CD73-PE flow cytometry analysis plot (specific staining in blue, isotype control staining in red) on unsorted, and MAC-sorted CD73+ and CD73– fractions from D120 organoids showing the percentage of CD73+ cells.

(B) Immunofluorescence analysis of PR markers CRX and RECOVERIN in dissociated cells from D120 organoids (unsorted fraction) and in CD73+ and CD73– fractions after MACS.

(C) Immunolabeling of RECOVERIN+ cells in unsorted, and sorted CD73+ and CD73– fractions from D140 AAVS1:*CrxP*_H2BmCherry retinal organoids.

(D) Exclusive expression of CRX and PAX6 in dissociated cells from D120 organoids (unsorted) and after MACS targeting CD73 (positive).

(E) qRT-PCR expression analysis of PR-specific genes in cells from unsorted (gray), and CD73+ (red) and CD73– (blue) fractions after MACS at D120 (mean ± SD; n = 25 organoids from N = 6 differentiations, *p < 0.05, **p < 0.01, multiple comparisons Kruskal-Wallis test). Gene expression is indicated relative to organoids at D120.

(F) Quantitative analysis by flow cytometry of apoptotic (PI+) cells on unsorted and CD73+ fractions in dissociated cells from: unfrozen retinal organoids (unsorted and CD73+ fresh), freeze-thawed CD73+ cells, freeze-thawed retinal organoids (unsorted and CD73+ freeze-thawed organoids) (*p < 0.05, multiple comparisons Kruskal-Wallis test).

(G) Co-expression of CRX and RECOVERIN in unsorted or sorted CD73+ cells from dissociated freeze-thawed organoids.

Scale bars, 50 μm (B), 25 μm (C, D, and G).

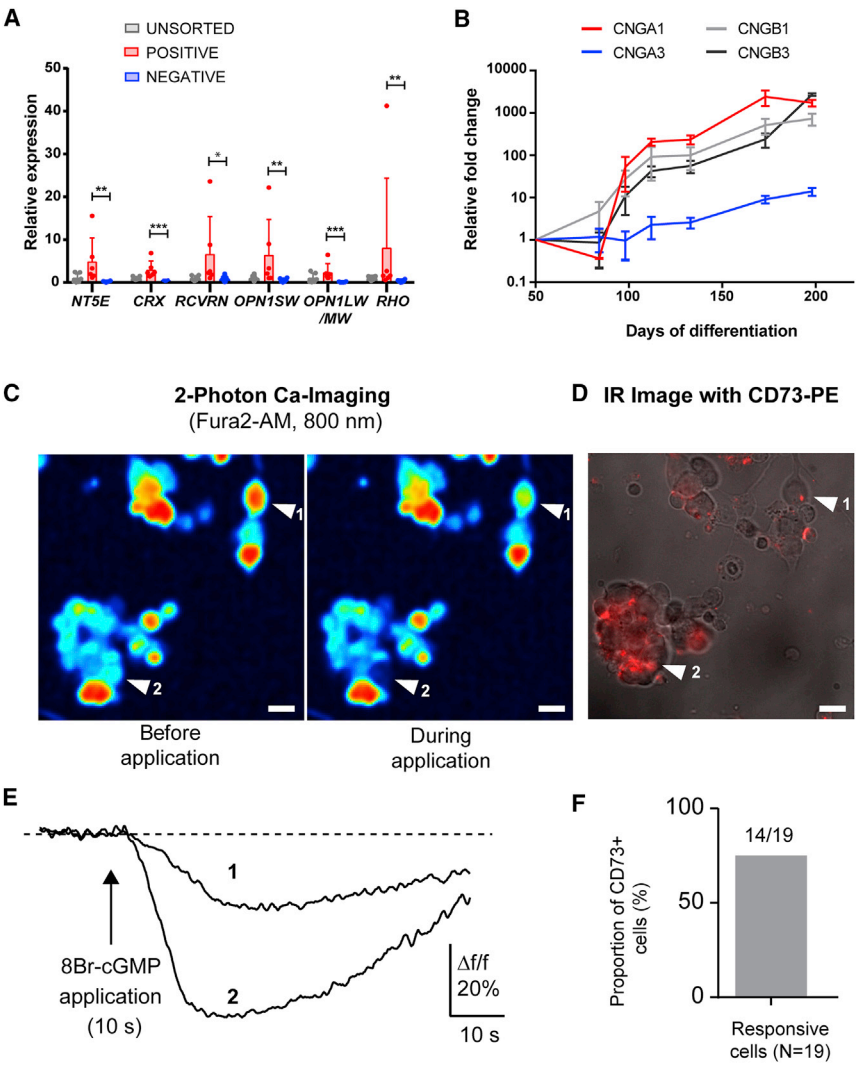


**Figure 3. Characterization of CD73+ Cells from Mature Retinal Organoids**

(A) qRT-PCR expression analysis of PR-specific genes in cells from unsorted (gray), and CD73+ (red) and CD73– (blue) fractions after MACS at D200 (mean ± SD; n = 25 organoids from N = 6 differentiations, *p < 0.05, **p < 0.01, **p < 0.001, multiple comparisons Kruskal-Wallis test). Gene expression is indicated relative to organoids at D200.

(B) qRT-PCR time course analysis of CNG channel subunits in organoids between D50 and D200 (mean ± SD; n = 5 organoids from N = 3 differentiation per time point). Gene expression at each time point is indicated relative to organoids at D50.

(C) Representative examples of 2-Photon Fura2-AM fluorescence images (calcium imaging) obtained before (left) and during (right) application of 8-Br-cGMP on dissociated retinal cells at D190. White arrows 1 and 2 represent two responsive cells.

(D) Infra-red (IR) image showing CD73-PE staining on dissociated retinal cells at D190. White arrows indicate responsive cells denoted 1 and 2 from image (C).

(E) Fluorescence traces after application of cGMP analog on cells 1 and 2 displayed in (C and D), expressed as percentage change from baseline fluorescence (Δf/f%).

(F) Percentage of CD73+ cells among the 8-Br-cGMP-responsive cell population (n = 19 from N = 5).

Scale bars, 10 μm (C and D).

organoids containing mature rods and cones (Reichman et al., 2014, 2017). qRT-PCR analysis clearly showed a significant overexpression of both mature cone- (*OPN1SW* and *OPN1LW/M*) and rod-specific (*RHO*) genes in CD73+ cells compared with CD73– cells (Figures 3A and S3B), in agreement with previous immunostaining data revealing the co-expression of CD73 with CONE ARRESTIN, BLUE OPSIN, and RED/GREEN OPSIN in retinal organoids (Reichman et al., 2017). The increased expression of *NT5E*, as well as *CRX* and *RCVRN*, in the CD73– positive fraction, confirmed the efficacy of the MACS process in retinal organoids from mature stages (Figures 3A and S3B). qRT-PCR analysis of the different subunits of cyclic nucleotide-gated ion (CNG) channels, expressed in functional PRs, showed that the expression of both rod-specific CNG channel subunits (CNGA1 and CNGB1) and of cone-specific CNG channel subunits (CNGA3 and CNGB3) started between D50 and D100 and increased after D150 (Figure 3B). To assess whether the functionality of CD73+ cells was consistent with PR electrophysiological behavior, we studied CNG channel activity in dark-like conditions in adherent cultures of dissociated retinal organoids. By combining live two-photon calcium imaging with infrared imaging, we monitored in CD73+ cells, labeled with a PE-conjugated CD73 antibody, the variations in intracellular $Ca^{2+}$ levels in response to the addition of a cGMP analog (8-Br-cGMP), as described previously (Mellough et al., 2015; Reichman et al., 2017). As dissociated cells from D120 organoids did not show any functional response (data not shown), experiments were performed in D190 dissociated cells when the expression of all subunits is optimal. Fura-2-loaded cells showed an increase in intracellular $Ca^{2+}$ when exposed to 8-Br-cGMP, as demonstrated by decreased intracellular fluorescence

(−22.42% ± 2.67%, n = 34, N = 8) (Figures 3C–3E). More importantly, the majority of the responsive cells were CD73– PE+ cells (Figure 3F). Consistently with their gene expression profile, CD73+ cells displayed a PR-specific response to the cGMP analog, supporting the use of CD73 as a marker of the PR cell population.

### Safety Assessment of hiPSC-Derived Retinal Cells

Since the use of PSC-derived cells is associated with the risk of the presence of potentially tumorigenic undifferentiated cells (Tucker et al., 2011), we evaluated by immunofluorescence the presence of residual undifferentiated PSCs and mitotic cells in retinal organoids. No expression of pluripotency markers OCT4, NANOG, or SSEA-4 were detected in dissociated retinal cells from D120 organoids, excluding the presence of undifferentiated PSCs. In contrast to undifferentiated hiPSC colonies (Figure 4A), very few cells were positive for the mitotic marker Ki67 at D120, corresponding to remaining retinal progenitor cells (Figure 4B). These data demonstrated the rarity of proliferative cells already before the selection of the PR by MACS. The safety of both unsorted and sorted CD73+ cells was assessed by transplanting 300,000 unsorted cells or MAC-sorted CD73+ cells from D120 organoids in the SRS of adult immunodeficient NUDE rats. As expected, no hyper-proliferation was observed after 8 weeks in animals engrafted with differentiated retinal cells (Figure 4C). Half of the NUDE rats transplanted with undifferentiated hiPSCs developed tumors in the eye (Figure 4D). Immunostaining with antibodies specifically directed against a cytoplasmic (STEM 121) or a human nuclear antigen (HNA) demonstrated the presence of human cells in the SRS 8 weeks after transplantation with both unsorted and sorted CD73+ cells (Figures 4E and 4F). The absence of Ki67+ cells in the SRS confirmed that both transplanted unsorted and CD73+ cells do not contain mitotically active cells (Figure 4F), confirming that retinal cells derived from D120 organoids are suitable for safe transplantation studies.

### Transplantation of Unsorted and CD73+ Cells into the Dystrophic P23H Rat Retina

Next, we sought to study the transplantation competence of CD73+ cells in a host environment recapitulating degenerative conditions. The P23H transgenic rat, which carries a P23H mutated *Rhodopsin* transgene, is a well-characterized model of rod-cone dystrophies, displaying progressive PR degeneration starting from 1 month after birth (Orhan et al., 2015). We transplanted unsorted retinal cells or sorted CD73+ cells from D120 organoids into 6-week-old hemizygous P23H rats, corresponding to an intermediate stage of PR degeneration (Orhan et al., 2015). One week after transplantation, unsorted cells survived in the SRS, identified by the expression of human-specific markers, STEM121, HNA, and human cytochrome *c* oxidase (MTCO2) (Figure 5A). hiPSC-derived retinal cells do not seem to migrate into the host ONL. Instead, S121+ cells were densely packed in the SRS, forming a new distinct layer of cells between host PRs and RPE even 4 weeks after transplantation (Figures 5B and 5C). Interestingly, the primary antibody against RECOVERIN, directed against an epitope of the human protein, led to a stronger signal against human cells than against host rat PRs and bipolar cells (Figure 5C). Although the RECOVERIN staining in the rat retina was still clearly detectable and highly specific (Figure 5D), this difference in the signal intensity can be used as an additional strategy to distinguish the xeno-transplant. Another parameter allowing for a straightforward identification of transplanted cells was the striking difference in the size and heterochromatin distribution of the nuclei in rat and human PRs. Consistent with previous observations (Gonzalez-Cordero et al., 2017), human nuclei were bigger in size (Figure 5E) with multiple chromocenters (Solovei et al., 2009); conversely rat PRs had smaller nuclei and highly condensed heterochromatin at their center (Figure 5E). While a large part of human transplanted cells stained with anti-RECOVERIN antibody, double S121+/PAX6+ cells were also detected (Figure 5F), confirming the heterogeneous identity of unsorted cells.

In contrast to unsorted cells, xeno-grafts with CD73+ cells gave rise to a homogeneous population of cells, co-expressing S121 and RECOVERIN (Figure 6A) and completely devoid of PAX6+ cells 4 weeks after transplantation (Figure 6B). Further characterization of grafted CD73+ cells showed a high enrichment in cones, stained by human-specific CONE ARRESTIN (hCAR) antibody, while only few RHODOPSIN+ cells were detected (Figure 6C). hCAR+ cells corresponded predominantly to red/green cones (Figure 6D) and few human HNA+ cones expressed BLUE OPSIN (Figure 6E). When the host PRs are mostly degenerated in some animals, human PRs could be directly in contact with the host inner nuclear layer (INL), and the expression of the pre-synaptic protein RIBEYE could be observed as immunoreactive spots, distributed at the extremities of hCAR+ cells (Figure 6F). Immunostaining with PKCα antibody allowed the visualization of tight apposition between human S121+ cells and PKCα+ bipolar cells 4 weeks after transplantation (Figures 6G and 6G′).

In a few animals (n = 2/7) we observed, at 10 weeks post-transplantation, clusters of human PRs co-expressing S121 and RECOVERIN intercalated in the host retina (Figure 7A), indicating the ability of CD73+ cells to survive for a relatively long time in the presence of immunosuppressive treatment. The limited efficacy of the immunosuppressive regimen and possible blood-retina barrier damage subsequent to surgery could explain the limited number of animals in which human cells can be detected 10 weeks

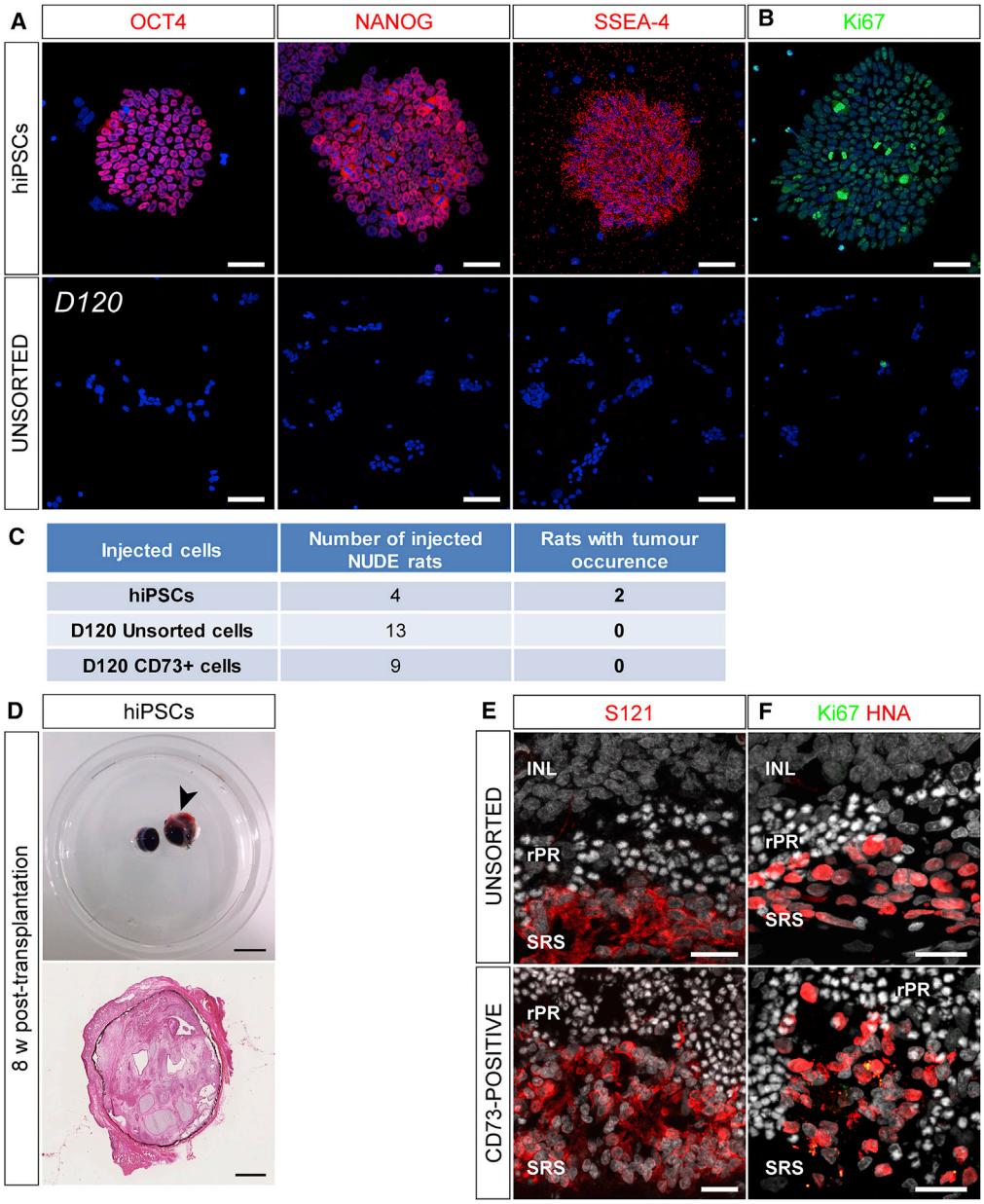


**Figure 4. Safety Assessment of hiPSC-Derived Retinal Cells**

(A) Immunostaining showing the expression of pluripotency markers OCT4, NANOG, and SSEA-4 in iPSC colonies (hiPSCs) but not in dissociated cells (unsorted) from D120 retinal organoids.

(B) Immunolabeling for Ki67 protein, associated with cell proliferation, in a representative iPSC colony and dissociated cells from D120 retinal organoids. Note loss of Ki67 expression in retinal cells.

(C) Table recapitulating the tumorigenicity test after subretinal transplantation into NUDE rats of dissociated hiPSCs and D120 unsorted or MAC-sorted CD73+ cells. Observations were made 8 weeks after the transplantation.

(D) Example of eyeballs of NUDE rats 8 weeks after subretinal transplantation of hiPSCs (black arrow) compared with non-transplanted eye. Bottom panel illustrates H&E staining of cross-section of the same hiPSC-transplanted eye.

(E) Representative confocal images showing the presence of human S121+ cells in the SRS of NUDE rat 8 weeks after transplantation of D120 unsorted cells or MAC-sorted CD73+ cells. Nuclei were counterstained with DAPI (gray).

(F) Absence of double Ki67+/HNA+ cells in unsorted and sorted CD73+ grafted cells 8 weeks after transplantation. Nuclei were counterstained with DAPI (gray). Scale bars, 1 cm (D) (top panel), 1 mm (D) (bottom panel), 50 μm (A and B), 20 μm (E and F). SRS, subretinal space; rPR, rat photoreceptors.

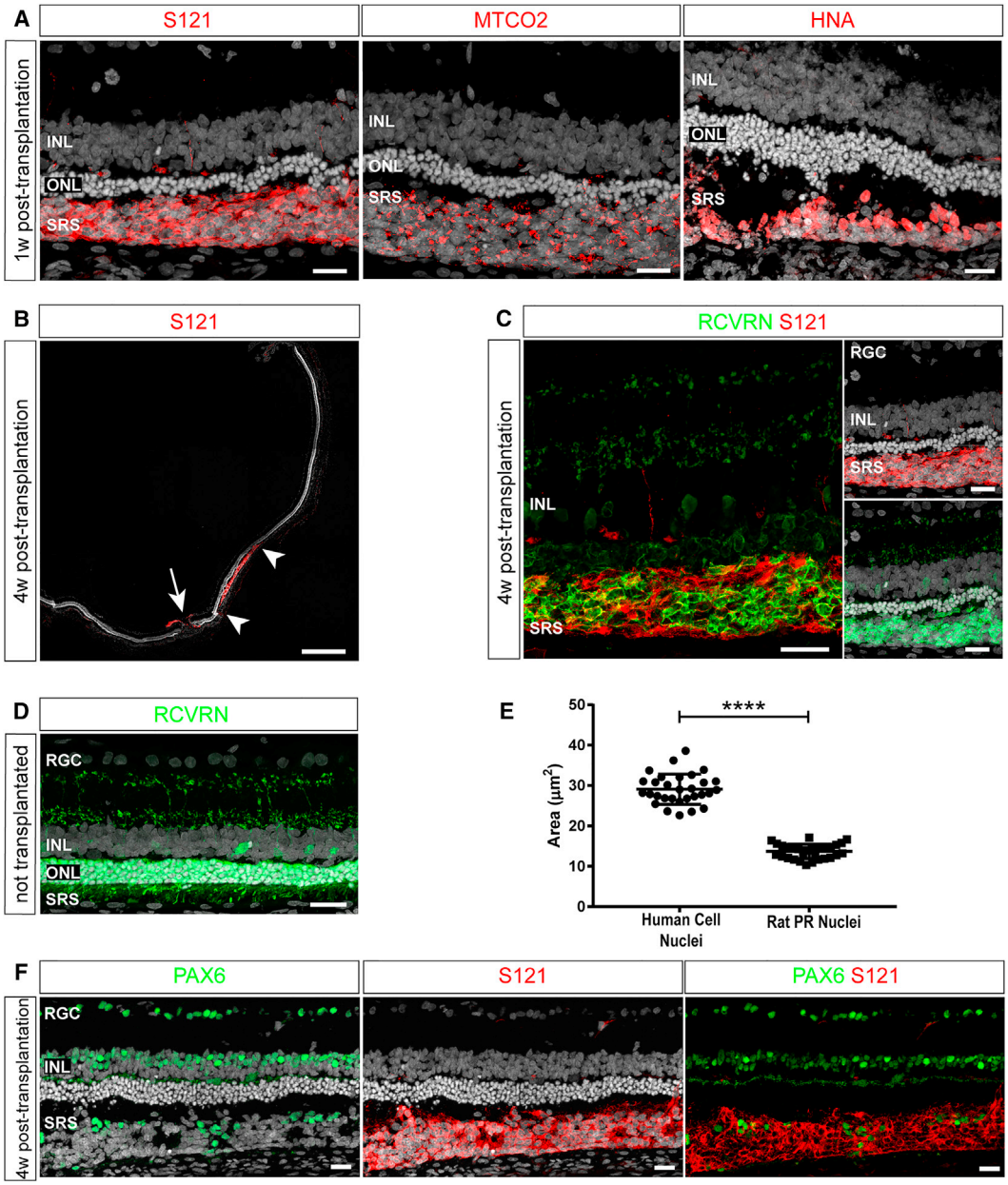


**Figure 5. Transplantation of hiPSC-Derived Retinal Cells into a Rat Model of Retinal Degeneration**

(A) Identification of donor human cells 1 week after transplantation by using three different human-specific antibodies (red): STEM 121 (left), MTCO2 (center), and HNA (right).

(B) Confocal mosaic image of D120 unsorted cell-transplanted eye showing the distribution of human S121+ cells in the SRS 4 weeks after transplantation. Arrowheads delimitate the spread of the grafted cells; the site of injection is indicated with an arrow.

(C) Most transplanted human retinal cells (S121+ cells) coexpress RECOVERIN. Note that RECOVERIN staining is lower in rat cells than in human cells.

(D) Example of RECOVERIN immunostaining in a non-grafted retina from P23H rat at 10 weeks of age. RECOVERIN antibody specifically labels rat PRs and part of the bipolar cells within the INL.

(E) Size of nuclei area of transplanted human cells and endogenous rat PRs 4 weeks after transplantation (mean ± SD, n = 30 nuclei measured, N = 3 grafted retinas; ****$p < 0.0001$, Mann-Whitney test).

(F) Some transplanted human S121+ retinal cells express the transcription factor PAX6.

Nuclei were counterstained with DAPI (gray). Scale bars, 20 μm (A, C, D, and F), 500 μm (B). SRS, subretinal space; ONL, outer nuclear layer, INL, inner nuclear layer; RGC, retinal ganglion cell layer.

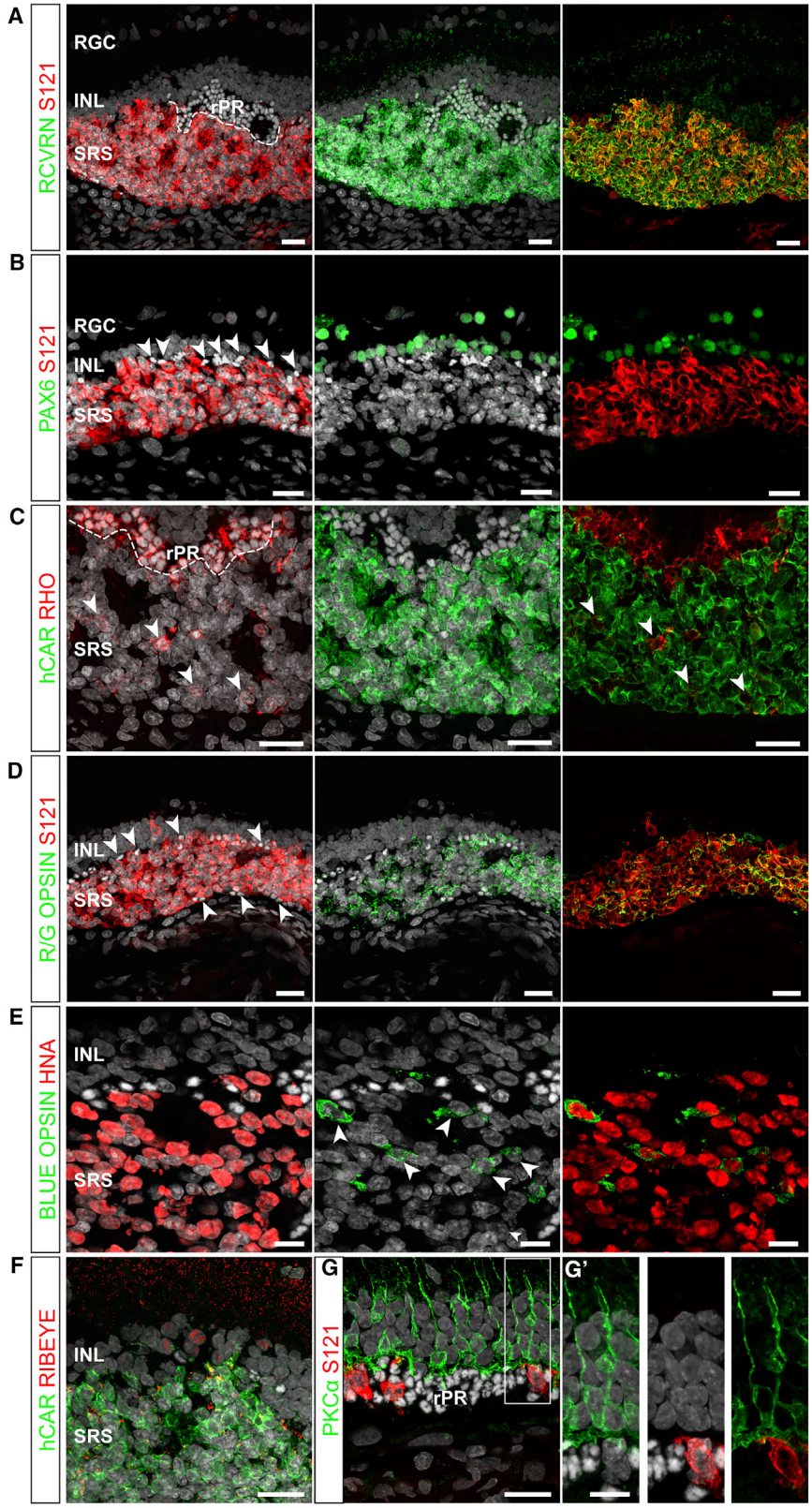


**Figure 6. Transplantation of hiPSC-Derived CD73+ Photoreceptors into the P23H Rat Model of Retinal Degeneration**

(A) Human S121+ cells co-expressing PR marker REVOVERIN located in close proximity to the rat INL. The residual rat PRs are delimited by the white dotted line.

(B) Absence of double S121/PAX6-positive cells. Transplanted CD73+ cells labeled by S121 are in close proximity with host PAX6+ cells within the INL. Arrowheads indicate residual rat PR nuclei.

(C) Labeling of human cone PRs by human-specific CONE ARRESTIN antibody (hCAR) and rod PRs by RHODOSPIN antibody. Arrowheads indicate human RHODOSPIN+ cells. Residual rat Rhodopsin+ PRs are delimited by the white dotted line.

(D) Human S121+ cells co-expressing cone PR marker R/G OPSIN. Residual S121– rat PRs (arrowheads) can be recognized by their nuclei features (smaller size and brightness).

(E) Some human HNA+ cells express blue cone marker BLUE OPSIN (arrowheads).

(F) Staining for synaptic protein RIBEYE and human CONE ARRESTIN (hCAR) showing localized punctate RIBEYE expression in human cone PRs directly in contact with the INL.

(G) Rat PKCα+ bipolar cells are in close proximity to human S121+ cells inserted within the host ONL. The area delimited by the line indicates the location of high-magnification images presented in (G').

All observations were made 4 weeks after transplantation. Nuclei were counterstained with DAPI (gray). Scale bars, 20 μm (A–D), 10 μm (E–G'). SRS, subretinal space; rPR, rat photoreceptors; INL, inner nuclear layer; RGC, retinal ganglion cell layer.

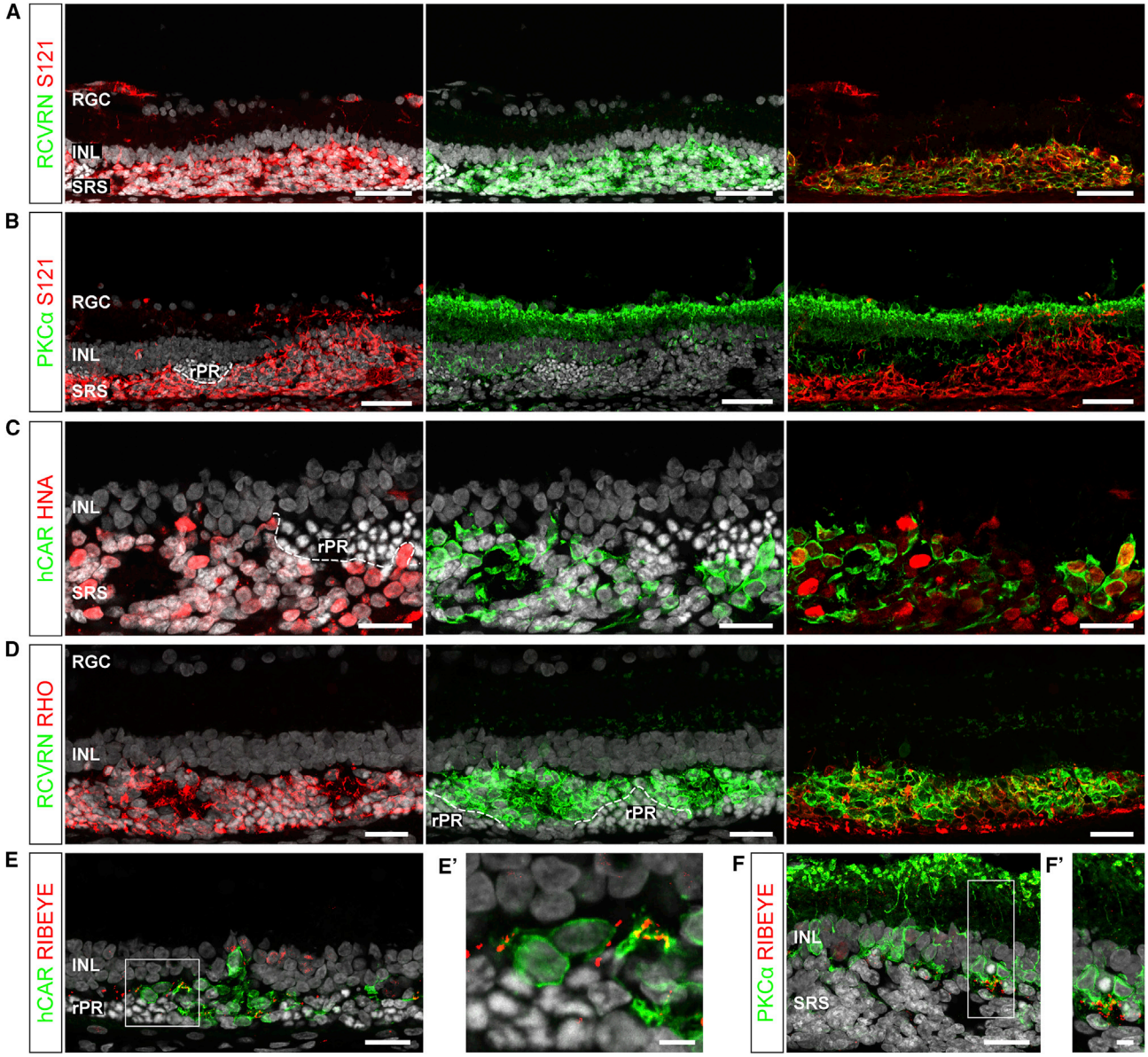


**Figure 7. Long-Term Survival of Transplanted CD73+ Cells**

(A) CD73+ human PRs, co-expressing S121 and RECOVERIN, are intercalated within the rat retina.

(B) Example of the distribution of human S121+ cells in close proximity to rat PKCα+ bipolar cells.

(C) Transplanted PRs co-expressing human CONE ARRESTIN (hCAR) and human marker HNA. The residual rat PRs are delimited by the white dotted line.

(D) Staining for human and rat rod PRs with RHODOPSIN and RECOVERIN antibodies.

(E) RIBEYE protein expression in the rat outer plexiform layer close to human cone PRs (hCAR+ cells). The area delimited by the line indicates the location of the high-magnification image presented in (E′).

(F) RIBEYE protein expression in close proximity to the synaptic terminals of rat PKCα+ bipolar cells. The area delimited by the line indicates the location of the high-magnification image presented in (F′).

All observations were made 10 weeks after transplantation. Nuclei were counterstained with DAPI (gray). Scale bars, 50 μm (A and B), 20 μm (C–E and F), 5 μm (E′ and F′). SRS, subretinal space; rPR, rat photoreceptors; INL, inner nuclear layer; RGC, retinal ganglion cell layer.

after transplantation. Human S121+ PRs were located in close proximity to the rat PKCα+ bipolar cells (Figure 7B). As in xeno-grafts analyzed 4 weeks after transplantation (Figure 6), again a large part of transplanted human HNA+ cells corresponded to cones (hCAR+ cells), even though few rods co-expressing bright RECOVERIN and RHODOPSIN can be observed (Figures 7C and 7D). Interestingly, some of the transplanted hCAR+ cones closest to the host INL expressed the pre-synaptic marker RIBEYE (Figures 7E and 7E′). Consistently, some of the rat PKCα+ bipolar cells closest to the human cells, distinguishable by their nuclear morphology, expressed RIBEYE at their synaptic terminals extending into the outer plexiform layer (Figures 7F and F′).

## DISCUSSION

In this study, we have developed a strategy based on the MACS of CD73+ cells to efficiently isolate PRs from hiPSC-derived retinal organoids and we demonstrated that CD73+ PR precursors could be safely transplanted into a host retina. One of the major challenges ahead for the development of a stem cell-based therapy to replace PRs is to obtain a consistent cell therapy product by complying with GMP guidelines, with no variations in terms of purity, yields, and quality of the manufactured cells. Using our retinal differentiation protocol combined with CD73– cell sorting, we obtained a large number of cells corresponding to a homogeneous population of PR precursors, as shown by *in vitro* and *in vivo* characterization. Our differentiation protocol is based on a feeder-free iPSC culture system and uses exclusively chemically defined xeno-free compounds. GMP-compliant MACS enrichment is already used in clinical trials (Menasché et al., 2015), with no negative impact or long-term side effects due to the microbeads at the surface of MAC-sorted cells (Handgretinger et al., 1998). Thus, our entire protocol to manufacture a cell therapy product should be easily GMP transferable. Moreover, MACS could be performed using cryopreserved organoids, ensuring the possibility to store the organoids at the appropriate stage of differentiation for downstream applications.

Despite a reasonable variability, an adequate number of viable CD73+ cells for transplantation can be still isolated by MACS. Starting from 20 million dissociated retinal cells at D120 of differentiation, MACS yielded 5 ± 1.8 million CD73+ cells, corresponding to the 25% ± 9% of the total cell population, demonstrating that large-scale production of a homogeneous PR precursor cell population can be reached. We proposed that 120-day-old retinal organoids represent the most suitable source of transplantable PRs, since at this stage the CD73+ cell population is mostly composed of immature PRs expressing CRX and RECOVERIN, but not OPSIN and RHODOPSIN. The precise definition of the ontogenetic stage of donor cells is very important for transplantation success, as previously demonstrated in mice, where only early post-natal PR precursors are able to efficiently integrate into the retina (Pearson et al., 2012; Waldron et al., 2017). The temporal profile of the expression of PR genes in our retinal organoids is very similar to the profile recently reported in human fetal retina (Hoshino et al., 2017; Welby et al., 2017). Also, expression of genes in D115-D136 human fetal retina was correlated to mouse P2-P4 retina in a comparative analysis of human and mouse transcriptome during retinal development (Hoshino et al., 2017), corroborating our choice of the differentiation stage of hiPSC-derived retinal organoids to isolate transplantable PR precursors. Recent transcriptome analysis of developing human PRs derived from PSCs should be also helpful for the isolation of PSC-derived PRs at the right stage of development, compatible for future transplantation studies (Kaewkhaw et al., 2015; Phillips et al., 2017; Welby et al., 2017).

One major advantage of the separation strategy presented here relies on the targeting of one single-cell surface antigen, CD73. Positive selection of retinal cells expressing CD73 has been mainly focused on rods, using Nrl:GFP mice or AAVs carrying a rhodopsin-driven GFP to specifically label rods (Eberle et al., 2011; Lakowski et al., 2011, 2015; Santos-Ferreira et al., 2016a). Nevertheless, CD73 has also been used for the enrichment of cone-like cells from a *Nrl−/−* mouse retina (Santos-Ferreira et al., 2015). Very recently, a comparative analysis of the transcriptome of human fetal and iPSC-derived cones, identified with the use of an AAV2/9-pR2.1:GFP reporter, and screening for cell surface-specific markers for cones in GFP+ cells, has been reported. Interestingly, *NT5E* (CD73) expression was not upregulated in GFP+ cones isolated by fluorescence-activated cell sorting (FACS) (Welby et al., 2017). This may be explained by the fact that CD73 is expressed by both rods and cones. Hence, in the absence of rods, no overexpression of CD73 is expected. Indeed, in our study, we found that hiPSC-derived retinal MAC-sorted CD73+ cells overexpress both rod- and cone-specific genes compared with CD73– cells.

Remarkably, the enrichment in PR precursors obtained after CD73-based MACS from D120 retinal organoids is in agreement with recent data reported on human retinal tissues (Lakowski et al., 2018). Indeed, FACS for CD73 from fetal retinae after 14 weeks of gestation allowed an enrichment for PRs, despite a large variability between different fetal samples (50% ± 24%). The ontogenetic stage of retinal organoids is critical for CD73-based PR selection, since previous RNA sequencing analysis in CRX-GFP+ cells isolated from hESC-derived retinal organoids younger than

90 days failed to identify CD73 as a marker of early PR precursors (Kaewkhaw et al., 2015).

Transplantation studies demonstrated that CD73-sorted PR precursors survive and mature into normal and degenerating rat retinae during several weeks. Surprisingly, a large part of transplanted CD73+ cells could be identified as cones in the SRS of P23H rats, suggesting that exogenous factors present within the host retina may favor either differentiation or survival of cones. Another explanation may reside in the temporal window of CD73 sorting, which may correspond to the peak of cone generation. Previous transplantation studies in mouse degenerative models had reported the presence of hiPSC-derived PRs within host mouse ONL, identified by GFP expression obtained via viral labeling (Gonzalez-Cordero et al., 2017; Lamba et al., 2009; Zhu et al., 2017). Gonzalez-Cordero and colleagues were able to confirm the human origin of most of the virally labeled human PSC-derived PRs by immunostaining with human-specific nuclear antigen. Importantly, they also reported the presence of small numbers of GFP+/HNA– within host ONL, whose morphology closely resembled that of mouse PRs, thereby demonstrating for the first time that human PSC-derived PRs can also engage in cytoplasmic material transfer following transplantation (Gonzalez-Cordero et al., 2017). The absence of a morphological difference between human GFP+ cells and mouse PRs may lead to a reconsideration of the human identity of GFP+ cells in previous studies (Lamba et al., 2009; Zhu et al., 2017). Donor-host cytoplasmic exchange has never been reported in transplantation studies in the rat retina. In our study, transplanted human PRs can be clearly distinguished from rat PRs thanks to both specific immunolabeling and cytological features. Remarkably, no HNA+ or S121+ cell displaying nuclear morphology peculiar to rat PRs was detected in host eyes, suggesting that transfer of cytoplasmic material between donor CD73+ PRs and host rat PRs does not seem to occur in the animal model presented here. Nevertheless, further studies would be necessary to undoubtedly exclude this process in the rat retina.

Despite the ability of CD73+ PRs to specifically respond to cGMP *in vitro,* no significant functional improvement was detected by electroretinography in P23H rats transplanted with unsorted or CD73+ cells compared with untreated eyes. Since human PRs were incorporated in a small area of the retina, more suitable strategies should be applied to determine the functionality of transplanted CD73+ cells. Also, in light of recent findings highlighting the structural divergence between rodent and human in proteins essential to PR synaptogenesis (Laver and Matsubara, 2017), more closely related species such as non-human primates would be more appropriate to evaluate the efficacy of human PR grafts.

In summary, we have reported the generation and the separation of an hiPSC-derived PR precursor cell population amenable to GMP manufacturing and compatible for future cell replacement therapy. The simplicity and the robustness of our separation strategy represent a reliable source to obtain PRs, not only in the context of cell replacement, but also for a broad spectrum of applications, such as disease modeling or drug screening.

## EXPERIMENTAL PROCEDURES

See Supplemental Experimental Procedures for detailed protocols and Supplemental Information for antibodies (Table S1) and qPCR probes (Table S2).

### MACS

Retinal organoids at various time points of differentiation were dissociated with papain (Worthington) according to the protocol described in Reichman et al. (2017). To remove residual aggregates, cell suspensions were filtered through a 30-μm strainer (Miltenyi Biotec). Dissociated cells were resuspended in MACS buffer and incubated first with CD73 antibody (BioLegend) for 10 min at 4°C at a dilution of 1:10 and then, after washing, with 20 μL of anti-mouse IgG1 MicroBeads (Miltenyi Biotec) per $10^7$ cells for 15 min at 4°C. Cells resuspended in 500 μL of MACS buffer were applied onto a pre-equilibrated mass spectrometry column fixed to a MACS separator (Miltenyi Biotec). The flow-through containing negative or unlabeled cells was collected by three washes with 500 μL MACS buffer. The positive fraction was eluted with 1 mL of MACS buffer following removal of the column from the magnet.

### Cell Transplantation

All protocols were approved by the local ethical committee (Charles Darwin ethical committee for animal experimentation C2EA-05) in strict accordance with French and European regulation for animal use in research (authorization number 05033). Cell suspension (4 μL) containing 300,000 cells in MACS buffer was injected with a trans-vitreal approach into the SRS of adult NUDE rats or 6-week-old hemizygous P23H rats. From 2 days before transplantation to the end of the follow-up, P23H rats were maintained under immunosuppression through cyclosporine treatment (210 mg/L) in the drinking water.

## SUPPLEMENTAL INFORMATION

Supplemental Information includes Supplemental Experimental Procedures, four figures, two tables, and one video and can be found with this article online at https://doi.org/10.1016/j.stemcr.2018.07.005.

## AUTHOR CONTRIBUTIONS

G.G. contributed to the conception, design, execution, and analysis/interpretation of all experiments and writing of the manuscript. K.B.M. contributed to surgery, histological processing, analysis of results, and revision of manuscript. A.C. performed calcium live imaging and analysis of results. A.S.-B. contributed to iPSC

culture and histological processing. J.-B.C. contributed to surgery. C.N. and O.R. contributed to iPSC culture. J.-A.S. contributed to administrative and financial support. J.D. contributed to analysis of calcium imaging. G.O. contributed to cell culture, clearing experiments, and revision of manuscript. S.R. contributed to interpretation of experiments and revision of manuscript. O.G. contributed to the conception, design, and interpretation of experiments, manuscript writing, and financial support.

## ACKNOWLEDGMENTS

We are grateful to J. Dégardin, M. Simonutti, and the staff of the Animal and Phenotyping facilities for help. We thank S. Fouquet from the Imaging facility, L. Riancho from the FACS facility, and A. Potey from the High Content Screening facility. We thank Dr. F. Sennlaub, X. Guillonneau, and Garita-Hernandez (Institut de la Vision, Paris) for helpful comments and Dr. C. Craft (Mary D. Allen Laboratory for Vision Research, USC ROSKI Eye Institute) for Cone arrestin antibody. This work was supported by grants from ANR (GPiPS: ANR-2010-RFCS005) (ANR-16-CE17-0008-02-SIGHTREPAIR), the Technology Transfer company SATT Lutech, LABEX REVIVE (ANR-10-LABX-73), and Retina France Association. This work was also performed in the frame of the LABEX LIFESENSES (ANR-10-LABX-65) within the Program Investissements d'Avenir (ANR-11-IDEX-0004-02). G.G. was a recipient of a PhD fellowship from the French Ministry of Higher Education and Research, K.B.M. was a recipient of a fellowship from the LABEX REVIVE (ANR-10-LABX-73), and O.R. was a recipient of a PhD fellowship from Fédération des Aveugles de France.

Received: March 7, 2018
Revised: July 9, 2018
Accepted: July 10, 2018
Published: August 9, 2018

## REFERENCES

Belle, M., Godefroy, D., Dominici, C., Heitz-Marchaland, C., Zelina, P., Hellal, F., Bradke, F., and Chedotal, A. (2014). A simple method for 3D analysis of immunolabeled axonal tracts in a transparent nervous system. Cell Rep. *9*, 1191–1201.

Dalkara, D., Goureau, O., Marazova, K., and Sahel, J.-A. (2016). Let there be light: gene and cell therapy for blindness. Hum. Gene Ther. *27*, 134–147.

Decembrini, S., Koch, U., Radtke, F., Moulin, A., and Arsenijevic, Y. (2014). Derivation of traceable and transplantable photoreceptors from mouse embryonic stem cells. Stem Cell Reports *2*, 853–865.

Decembrini, S., Martin, C., Sennlaub, F., Chemtob, S., Biel, M., Samardzija, M., Moulin, A., Behar-Cohen, F., and Arsenijevic, Y. (2017). Cone genesis tracing by the Chrnb4-EGFP mouse line: evidences of cellular material fusion after cone precursor transplantation. Mol. Ther. *25*, 634–653.

Eberle, D., Schubert, S., Postel, K., Corbeil, D., and Ader, M. (2011). Increased integration of transplanted CD73-positive photoreceptor precursors into adult mouse retina. Invest. Opthalmol. Vis. Sci. *52*, 6462.

Furukawa, A., Koike, C., Lippincott, P., Cepko, C.L., and Furukawa, T. (2002). The mouse Crx 5'-upstream transgene sequence directs cell-specific and developmentally regulated expression in retinal photoreceptor cells. J. Neurosci. *22*, 1640–1647.

Gonzalez-Cordero, A., West, E.L., Pearson, R.A., Duran, Y., Carvalho, L.S., Chu, C.J., Naeem, A., Blackford, S.J.I., Georgiadis, A., Lakowski, J., et al. (2013). Photoreceptor precursors derived from three-dimensional embryonic stem cell cultures integrate and mature within adult degenerate retina. Nat. Biotechnol. *31*, 741–747.

Gonzalez-Cordero, A., Kruczek, K., Naeem, A., Fernando, M., Kloc, M., Ribeiro, J., Goh, D., Duran, Y., Blackford, S.J.I., Abelleira-Hervas, L., et al. (2017). Recapitulation of human retinal development from human pluripotent stem cells generates transplantable populations of cone photoreceptors. Stem Cell Reports *9*, 820–837.

Handgretinger, R., Lang, P., Schumm, M., Taylor, G., Neu, S., Koscielnak, E., Niethammer, D., and Klingebiel, T. (1998). Isolation and transplantation of autologous peripheral CD34+ progenitor cells highly purified by magnetic-activated cell sorting. Bone Marrow Transplant. *21*, 987–993.

Hoshino, A., Ratnapriya, R., Brooks, M.J., Chaitankar, V., Wilken, M.S., Zhang, C., Starostik, M.R., Gieser, L., La Torre, A., Nishio, M., et al. (2017). Molecular anatomy of the developing human retina. Dev. Cell *43*, 763–779.e4.

Jayakody, S.A., Gonzalez-Cordero, A., Ali, R.R., and Pearson, R.A. (2015). Cellular strategies for retinal repair by photoreceptor replacement. Prog. Retin. Eye Res. *46*, 31–66.

Kaewkhaw, R., Kaya, K.D., Brooks, M., Homma, K., Zou, J., Chaitankar, V., Rao, M., and Swaroop, A. (2015). Transcriptome dynamics of developing photoreceptors in three-dimensional retina cultures recapitulates temporal sequence of human cone and rod differentiation revealing cell surface markers and gene networks. Stem Cells *33*, 3504–3518.

Lakowski, J., Han, Y.T., Pearson, R.A., Gonzalez-Cordero, A., West, E.L., Gualdoni, S., Barber, A.C., Hubank, M., Ali, R.R., and Sowden, J.C. (2011). Effective transplantation of photoreceptor precursor cells selected via cell surface antigen expression. Stem Cells *29*, 1391–1404.

Lakowski, J., Gonzalez-Cordero, A., West, E.L., Han, Y.T., Welby, E., Naeem, A., Blackford, S.J.I., Bainbridge, J.W.B., Pearson, R.A., Ali, R.R., et al. (2015). Transplantation of photoreceptor precursors isolated via a cell surface biomarker panel from embryonic stem cell-derived self-forming retina. Stem Cells *33*, 2469–2482.

Lakowski, J., Welby, E., Budinger, D., Di Marco, F., Di Foggia, V., Bainbridge, J.W.B., Wallace, K., Gamm, D.M., Ali, R.R., and Sowden, J.C. (2018). Isolation of human photoreceptor precursors via a cell surface marker panel from stem cell-derived retinal organoids and fetal retinae. Stem Cells *36*, 709–722.

Lamba, D.A., Karl, M.O., Ware, C.B., and Reh, T.A. (2006). Efficient generation of retinal progenitor cells from human embryonic stem cells. Proc. Natl. Acad. Sci. USA *103*, 12769–12774.

Lamba, D.A., Gust, J., and Reh, T.A. (2009). Transplantation of human embryonic stem cell-derived photoreceptors restores some visual function in Crx-deficient mice. Cell Stem Cell *4*, 73–79.

Laver, C.R.J., and Matsubara, J.A. (2017). Structural divergence of essential triad ribbon synapse proteins among placental mammals – implications for preclinical trials in photoreceptor transplantation therapy. Exp. Eye Res. *159*, 156–167.

Mandai, M., Fujii, M., Hashiguchi, T., and Sunagawa, G.A. (2017). iPSC-derived retina transplants improve vision in rd1 end-stage retinal-degeneration mice. Stem Cell Reports *8*, 69–83.

Mellough, C.B., Collin, J., Khazim, M., White, K., Sernagor, E., Steel, D.H.W., and Lako, M. (2015). IGF-1 signaling plays an important role in the formation of three-dimensional laminated neural retina and other ocular structures from human embryonic stem cells. Stem Cells *33*, 2416–2430.

Menasché, P., Vanneaux, V., Hagège, A., Bel, A., Cholley, B., Cacciapuoti, I., Parouchev, A., Benhamouda, N., Tachdjian, G., Tosca, L., et al. (2015). Human embryonic stem cell-derived cardiac progenitors for severe heart failure treatment: first clinical case report. Eur. Heart J. *36*, 2011–2017.

Meyer, J.S., Shearer, R.L., Capowski, E.E., Wright, L.S., Wallace, K.A., McMillan, E.L., Zhang, S.-C., and Gamm, D.M. (2009). Modeling early retinal development with human embryonic and induced pluripotent stem cells. Proc. Natl. Acad. Sci. USA *106*, 16698–16703.

Nakano, T., Ando, S., Takata, N., Kawada, M., Muguruma, K., Sekiguchi, K., Saito, K., Yonemura, S., Eiraku, M., and Sasai, Y. (2012). Self-formation of optic cups and storable stratified neural retina from human ESCs. Cell Stem Cell *10*, 771–785.

Orhan, E., Dalkara, D., Neuillé, M., Lechauve, C., Michiels, C., Picaud, S., Léveillard, T., Sahel, J.A., Naash, M.I., LaVail, M.M., et al. (2015). Genotypic and phenotypic characterization of P23H line 1 rat model. PLoS One *10*, e0127319.

Ortin-Martinez, A., Tsai, E.L.S., Nickerson, P.E., Bergeret, M., Lu, Y., Smiley, S., Comanita, L., and Wallace, V.A. (2017). A reinterpretation of cell transplantation: GFP transfer from donor to host photoreceptors. Stem Cells *35*, 932–939.

Osakada, F., Ikeda, H., Mandai, M., Wataya, T., Watanabe, K., Yoshimura, N., Akaike, A., Sasai, Y., and Takahashi, M. (2008). Toward the generation of rod and cone photoreceptors from mouse, monkey and human embryonic stem cells. Nat. Biotechnol. *26*, 215–224.

Pearson, R.A., Barber, A.C., Rizzi, M., Hippert, C., Xue, T., West, E.L., Duran, Y., Smith, A.J., Chuang, J.Z., Azam, S.A., et al. (2012). Restoration of vision after transplantation of photoreceptors. Nature *485*, 99–103.

Pearson, R.A., Gonzalez-Cordero, A., West, E.L., Ribeiro, J.R., Aghaizu, N., Goh, D., Sampson, R.D., Georgiadis, A., Waldron, P.V., Duran, Y., et al. (2016). Donor and host photoreceptors engage in material transfer following transplantation of post-mitotic photoreceptor precursors. Nat. Commun. *7*, 13029.

Phillips, J., Jiang, P., Howden, S., Barney, P., Min, J., York, N., Chu, L., Capowski, E., Cash, A., Jain, S., et al. (2017). A novel approach to single cell RNA-sequence analysis facilitates in silico gene reporting of human pluripotent stem cell-derived retinal cell types. Stem Cells *36*, 1–16.

Reichman, S., Terray, A., Slembrouck, A., Nanteau, C., Orieux, G., Habeler, W., Nandrot, E.F., Sahel, J.-A., Monville, C., and Goureau, O. (2014). From confluent human iPS cells to self-forming neural retina and retinal pigmented epithelium. Proc. Natl. Acad. Sci. USA *111*, 8518–8523.

Reichman, S., Slembrouck, A., Gagliardi, G., Chaffiol, A., Terray, A., Nanteau, C., Potey, A., Belle, M., Rabesandratana, O., Duebel, J., et al. (2017). Generation of storable retinal organoids and retinal pigmented epithelium from adherent human iPS cells in xeno-free and feeder-free conditions. Stem Cells *35*, 1176–1188.

Santos-Ferreira, T., Postel, K., Stutzki, H., Kurth, T., Zeck, G., and Ader, M. (2015). Daylight vision repair by cell transplantation. Stem Cells *33*, 79–90.

Santos-Ferreira, T., Völkner, M., Borsch, O., Haas, J., Cimalla, P., Vasudevan, P., Carmeliet, P., Corbeil, D., Michalakis, S., Koch, E., et al. (2016a). Stem cell-derived photoreceptor transplants differentially integrate into mouse models of cone-rod dystrophy. Invest. Ophthalmol. Vis. Sci. *57*, 3509–3520.

Santos-Ferreira, T., Llonch, S., Borsch, O., Postel, K., Haas, J., and Ader, M. (2016b). Retinal transplantation of photoreceptors results in donor–host cytoplasmic exchange. Nat. Commun. *7*, 13028.

Santos-Ferreira, T.F., Borsch, O., and Ader, M. (2017). Rebuilding the missing part—a review on photoreceptor transplantation. Front. Syst. Neurosci. *10*, 1–14.

Singh, M.S., Charbel Issa, P., Butler, R., Martin, C., Lipinski, D.M., Sekaran, S., Barnard, A.R., and MacLaren, R.E. (2013). Reversal of end-stage retinal degeneration and restoration of visual function by photoreceptor transplantation. Proc. Natl. Acad. Sci. USA *110*, 1101–1106.

Singh, M.S., Balmer, J., Barnard, A.R., Aslam, S.A., Moralli, D., Green, C.M., Barnea-Cramer, A., Duncan, I., and MacLaren, R.E. (2016). Transplanted photoreceptor precursors transfer proteins to host photoreceptors by a mechanism of cytoplasmic fusion. Nat. Commun. *7*, 13537.

Solovei, I., Kreysing, M., Lanctôt, C., Kösem, S., Peichl, L., Cremer, T., Guck, J., and Joffe, B. (2009). Nuclear architecture of rod photoreceptor cells adapts to vision in mammalian evolution. Cell *137*, 356–368.

Sridhar, A., Steward, M.M., and Meyer, J.S. (2013). Nonxenogeneic growth and retinal differentiation of human induced pluripotent stem cells. Stem Cells Transl. Med. *2*, 255–264.

Tucker, B.A., Park, I.H., Qi, S.D., Klassen, H.J., Jiang, C., Yao, J., Redenti, S., Daley, G.Q., and Young, M.J. (2011). Transplantation of adult mouse iPS cell-derived photoreceptor precursors restores retinal structure and function in degenerative mice. PLoS One *6*, e18992.

Tucker, B.A., Mullins, R.F., Streb, L.M., Anfnson, K., Eyestone, M.E., Kaalberg, E., Riker, M.J., Drack, A.V., Braun, T.A., and Stone, E.M. (2013). Patient-specific iPSC-derived photoreceptor precursor cells as a means to investigate retinitis pigmentosa. Elife *2013*, 1–18.

Waldron, P.V., Di Marco, F., Kruczek, K., Ribeiro, J., Graca, A.B., Hippert, C., Aghaizu, N.D., Kalargyrou, A.A., Barber, A.C., Grimaldi, G., et al. (2017). Transplanted donor- or stem cell-derived cone photoreceptors can both integrate and undergo material

transfer in an environment-dependent manner. Stem Cell Reports *10*, 1–16.

Welby, E., Lakowski, J., Di Foggia, V., Budinger, D., Gonzalez-Cordero, A., Lun, A.T.L., Epstein, M., Patel, A., Cuevas, E., Kruczek, K., et al. (2017). Isolation and comparative transcriptome analysis of human fetal and iPSC-derived cone photoreceptor cells. Stem Cell Reports *9*, 1898–1915.

Wiley, L.A., Burnight, E.R., DeLuca, A.P., Anfinson, K.R., Cranston, C.M., Kaalberg, E.E., Penticoff, J.A., Affatigato, L.M., Mullins, R.F., Stone, E.M., et al. (2016). cGMP production of patient-specific iPSCs and photoreceptor precursor cells to treat retinal degenerative blindness. Sci. Rep. *6*, 30742.

Zhao, C., Wang, Q., and Temple, S. (2017). Stem cell therapies for retinal diseases: recapitulating development to replace degenerated cells. Development *144*, 1368–1381.

Zhong, X., Gutierrez, C., Xue, T., Hampton, C., Vergara, M.N., Cao, L.-H., Peters, A., Park, T.S., Zambidis, E.T., Meyer, J.S., et al. (2014). Generation of three-dimensional retinal tissue with functional photoreceptors from human iPSCs. Nat. Commun. *5*, 1–14.

Zhu, J., Cifuentes, H., Reynolds, J., and Lamba, D.A. (2017). Immunosuppression via loss of IL2rγ enhances long-term functional integration of hESC-derived photoreceptors in the mouse retina. Cell Stem Cell *20*, 374–384.e5.